Vacancy-induced spin texture in a one-dimensional $S = \frac{1}{2}$ Heisenberg antiferromagnet

Sambuddha Sanyal, Argha Banerjee, and Kedar Damle
Department of Theoretical Physics, Tata Institute of Fundamental Research, Mumbai 400 005, India
(Received 15 August 2011; revised manuscript received 2 December 2011; published 21 December 2011)

We study the effect of a missing spin in a one-dimensional $S = 1/2$ antiferromagnet with nearest-neighbor Heisenberg exchange J and six-spin coupling $Q = 4qJ$ using quantum Monte-Carlo (QMC) and bosonization techniques. For $q < q_c \approx 0.04$, the system is in a quasilong range ordered power-law antiferromagnetic phase, which gives way to a valence-bond solid state that spontaneously breaks lattice translation symmetry for $q > q_c$. We study the ground-state spin texture $\Phi(r) = \langle G_\uparrow | S^z(r) | G_\uparrow \rangle$ in the the $S^z_{\rm tot} = 1/2$ ground state $|G_\uparrow\rangle$ of the system with a missing spin, focusing on the alternating part $N_z(r)$. We find that our QMC results for N_z at $q = q_c$ take on the scaling form expected from bosonization considerations, but violate scaling for $q < q_c$. Within the bosonization approach, such violations of scaling arise from the presence of a marginally irrelevant sine-Gordon interaction, whose effects we calculate using renormalization group (RG) improved perturbation theory. Our field-theoretical predictions are found to agree well with the QMC data for $q < q_c$.

DOI: 10.1103/PhysRevB.84.235129 PACS number(s): 75.10.Jm

I. INTRODUCTION

The one-dimensional $S = 1/2$ Heisenberg antiferromagnetic spin chain, with nearest-neighbour exchange couplings J is perhaps the simplest important model spin system in quantum magnetism. It has not only proved useful as a theoretical model for the magnetic properties of several Mott insulating materials,[1–3] but has also been the subject of many theoretical advances such as Bethe's original "Bethe ansatz" solution of this quantum many-body problem and later field-theoretical treatments that applied bosonization techniques to map the system to a $1 + 1$ dimensional bosonic field theory with a so-called "sine-Gordon" action, made up of a scale-invariant free-field part perturbed by a nonlinear cosine interaction.[4] In addition, the renormalization group (RG) analysis of the cosine interaction that perturbs the scale-invariant free-field action is a paradigmatic example of the treatment of "marginally irrelevant" interactions in the neighbourhood of a well characterized and tractable scale invariant RG fixed point.[5–10]

Such marginally irrelevant interactions can give rise to violations of scaling predictions at critical points due to the presence of logarithmic corrections that multiply the scaling answer. A well-known example is the O(N) critical point in four space-time dimensions.[11] In some other cases, such marginally irrelevant interactions give rise to *additive corrections* to scaling, which vanish logarithmically slowly. The one-dimensional Heisenberg chain displays both kinds of effects. For instance, gaps in the finite-size spectra of the spin-half chain are known to have additive logarithmic corrections that do not affect the leading behavior,[6] while the temperature dependence of the NMR relaxation rate $1/T_1$ violates scaling expectations due to the presence of an additional logarithmic factor in its temperature dependence.[12]

Similar logarithmic violations of scaling, arising from multiplicative logarithmic factors that multiply scaling predictions, have been argued to exist[13,14] in a much less well understood case of a two-dimensional $S = 1/2$ square lattice Heisenberg antiferromagnet on the verge of a continuous quantum phase transition[15,16] between the usual Néel ordered antiferromagnetic ground state and a spontaneously dimerized nonmagnetic state with valence-bond order. The underlying critical noncompact CP^1 (NCCP^1) field theory that has been proposed[15] as the continuum description of this transition is not as well understood from a RG standpoint, and since the numerics themselves are also more challenging, there have been some differences in the interpretation of these results.[17,18]

In our own recent work,[14] we have used extensive numerical computations to establish the presence of apparently logarithmic scaling violations in the impurity spin texture induced by a missing-spin defect at such a quantum critical point when the system has the usual SU(2) symmetry of spin rotations, and ascribed this effect to the presence of a yet-to-be-identified marginal operator at the putative NCCP^1 critical fixed point. In contrast, the corresponding spin texture in a system at an analogous critical point with enlarged SU(3) symmetry[20] was found to obey scaling predictions without any logarithmic violations,[19] suggesting that the underlying NCCP^2 critical point describing this SU(3) transition is free of such marginal operators. However, parallel work of Kaul[17] argues that such marginal operators would typically not lead to violations of scaling, and finds an alternative scenario more likely. In this alternative scenario, both the SU(2) and SU(3) transitions are described by fixed points with a leading irrelevant operator with small scaling dimension, and the violations of scaling arise from the fact that the quantity being studied depends *nonanalytically* on this leading irrelevant operator.

Here, we try and understand the origins of such multiplicative logarithmic corrections to impurity spin textures in the power-law Néel phase of the one-dimensional Heisenberg antiferromagnet. On the analytical side, we work within the bosonization framework and use RG improved perturbation theory to obtain predictions for the alternating part of the spin texture in this phase. These predictions are valid for any microscopic model in this power-law Néel ordered phase in one-dimension—this includes the experimentally relevant example of the Heisenberg spin chain with nearest-neighbor coupling J_1 and next-nearest-neighbor coupling J_2.

On the numerical side, for technical reasons which will be apparent below, we choose to compare these predictions with Quantum Monte Carlo (QMC) results for a somewhat

different microscopic model that has the same power-law Néel ordered phase in one dimension. This one-dimensional chain has a nearest neighbor Heisenberg exchange J and six-spin coupling $Q = 4qJ$. The Hamiltonian for this JQ_3 model is

$$H = -J \sum_{i=0}^{N} P_{i,i+1} - Q \sum_{i} P_{i,i+1} P_{i+2,i+3} P_{i+4,i+5}, \quad (1)$$

where $P_{ij} \equiv (\frac{1}{4} - \vec{S}_i \cdot \vec{S}_j)$ is the projector to the singlet state of the two spin-half variables at sites i and j, both J and Q are assumed positive, and we impose periodic boundary conditions by placing the system on a ring so that site $N + 1 + k$ is identified with site k (the total number of spins $N + 1$ is taken even).

From our QMC results, obtained using the singlet sector valence-bond projection method,[21] we find that the Q term drives a transition to a valence-bond solid phase at $q_c \approx 0.04$, so that the system is power-law Néel ordered for $q < q_c$, and valence-bond solid (VBS) ordered for $q > q_c$. Unlike the more well studied case in which such a transition is driven by next-nearest-neighbor Heisenberg antiferromagnetic exchange couplings, the present JQ_3 model does not have a sign problem in standard nonzero temperature QMC calculations (as well as in the ground-state projector QMC approach), and can therefore be studied at larger length scales and greater precision.

In order to explore the effects of vacancy defects, we remove the spin at site 0 and delete all interactions that involve this spin from our Hamiltonian. Since N is odd, the ground state of the chain with a missing spin is a doublet with $S_{\rm tot} = 1/2$. We focus on $|G_\uparrow\rangle$, the $S^z_{\rm tot} = 1/2$ component of this doublet, and compute the spin texture $\Phi(r) = \langle S^z(r)\rangle_\uparrow$ in this ground state for various values of q. This is done using a recently developed modification[22] of the singlet-sector projector QMC technique.[21] This spin texture can be decomposed as $\Phi(r) = \Phi_u(r) + (-1)^{r/a} N_z(r)$, where alternating part $N_z(r)$ and a uniform part $\Phi_u(r)$ are obtained from our numerical data by a suitable coarse-graining procedure.

These numerical results for $N_z(r)$ are compared to field theoretical calculations within the bosonization framework, keeping careful track of the effects of the marginal cosine interaction term using one-loop RG improved perturbation theory. Our basic conclusion is that this marginal cosine interaction does indeed lead to logarithmic violations of scaling by introducing logarithmic corrections that multiply the scaling predictions for N_z in the power-law Néel phase. Comparing these analytical predictions with our numerical results for $q < q_c$, we find good agreement with the data, with the strength of the logarithmic corrections being larger for q further away from the critical point and vanishing for $q = q_c$, as predicted by the bosonization approach.

The rest of this article is organized as follows. In Sec. II, we first summarize our approach to the analytical calculation of the ground-state spin texture induced by a missing spin, give our final predictions for the nature of the logarithmic violations of scaling, and discuss them from a somewhat more general RG standpoint. In Sec. III, we describe our projector QMC studies and compare the numerical data for N_z with our analytical predictions to establish our main results. We conclude with a discussion of the connection between our results and earlier work on vacancy effects in the NMR Knight shift and spin structure factor.

II. BOSONIZATION CALCULATION OF GROUND-STATE SPIN TEXTURE

A. Preliminaries

As is well known, we may model our one-dimensional magnet by the continuum effective Hamiltonian[4]

$$H = H_0 + H_1, \quad (2)$$

where the free field part H_0 is written as

$$H_0 = \frac{u}{2} \int_0^L dx \left[\left(\frac{d\phi}{dx}\right)^2 + \left(\frac{d\tilde{\phi}}{dx}\right)^2 \right], \quad (3)$$

and the interaction term H_1 reads

$$H_1 = -\frac{u\epsilon_0}{r_0^2} \int_0^L dx \cos\left[\frac{2\phi(x)}{R}\right], \quad (4)$$

here, r_0 is an ultraviolet regulator defined precisely later and

$$\frac{1}{2\pi R^2} = 1 - \pi\epsilon_0 \,. \quad (5)$$

The last constraint that relates R to the bare coupling constant ϵ_0 at scale r_0 arises from the SU(2) spin invariance of the underlying microscopic theory.[8] The well-known Kosterlitz-Thouless renormalization group theory[23] applied to the present SU(2) symmetric case yields the flow equation

$$\frac{d\epsilon}{d(\ln L)} = \beta_\epsilon[\epsilon(L)] \quad (6)$$

with the one loop expression for the beta function being given by[7]

$$\beta_\epsilon[\epsilon(L)] = 2\pi\epsilon^2(L) - \tfrac{1}{2}(2\pi)^2\epsilon^3(L) \,. \quad (7)$$

This equation can be solved to obtain the running coupling constant $\epsilon(L)$ at scale L as[7]

$$\frac{1}{\epsilon(L)} - \frac{1}{\epsilon_0} = -2\pi \left\{ \ln\left(\frac{L}{r_0}\right) + \frac{1}{2} \ln\left[\ln\left(\frac{L}{r_0}\right)\right] \right\} + \mathrm{O}(1) \,. \quad (8)$$

Note that ϵ_0 is *negative* in the power-law ordered antiferromagnetic phase in the present sign convention.

Within this bosonized formulation, the operator $S^z(r)$ at site $r = ja$ is represented as[24]

$$S^z(r) = \frac{a}{2\pi R} \frac{d\phi}{dr} + \frac{\mathcal{A}}{\sqrt{r_0}} (-1)^{\frac{r}{a}} \sin\left[\frac{\phi(r)}{R}\right]. \quad (9)$$

Here, the coefficient of the uniform part is fixed by SU(2) invariance while the coefficient of the alternating part is sensitive to microscopic details: $\mathcal{A} = \sqrt{a}c$ where a is lattice spacing of lattice model and c is a pure number that depends on the microscopic Hamiltonian.

Finally, we also recall that the one-point function $S = \langle \frac{1}{\sqrt{r_0}} \sin[\frac{\phi(r)}{R}] \rangle_\uparrow$ of the operator $\frac{1}{\sqrt{r_0}} \sin[\frac{\phi(r)}{R}]$ can be thought of as a function of L and the running coupling $\epsilon(L)$ for fixed

bare coupling ϵ_0 and fixed r/L. Thought of in this way, it obeys the Callan-Symanzik type equation,[7]

$$\left[\frac{\partial}{\partial \ln L} + \beta_\epsilon(\epsilon)\frac{\partial}{\partial \epsilon} + \gamma(\epsilon)\right] S\left[L, \epsilon(L) | \epsilon_0, \frac{r}{L}\right] = 0, \quad (10)$$

with the anomalous dimension having the expansion

$$\gamma(\epsilon) = \frac{1}{2} + \left(\frac{\pi}{2}\right)\epsilon(L) \quad (11)$$

in terms of the running coupling ϵ. As is well known, this can be solved to leading order in $\epsilon(L)$ to give the following scaling law for S:

$$S \cong \frac{F_0}{\sqrt{L}}\left[\frac{\epsilon_0}{\epsilon(L)}\right]^{\frac{1}{4}}[1 + \epsilon(L)R], \quad (12)$$

where $F_0\left(\frac{r}{L}\right)$ and $R\left(\frac{r}{L}\right)$ are some functions of the ratio $\frac{r}{L}$ and the key point about this formal expression for S is that all dependence on the ultraviolet regulator r_0 has been traded in for a dependence on $\epsilon(L)$, the running coupling at scale L for a flow that starts with bare coupling ϵ_0 at scale r_0.

B. Overview

With these preliminaries out of the way, we now outline the strategy used below to calculate the alternating part of $\langle S^z(r)\rangle_\uparrow$. The basic idea is to begin by calculating the result for this alternating part using the bosonized part of the alternating spin density and bare perturbation theory to first order in ϵ_0 for a finite system of length L. As we shall see below, this bare perturbation theory result will turn out to depend logarithmically on the value of the ultraviolet cutoff r_0 via a logarithmic ultraviolet divergence arising from a first-order perturbation theory contribution proportional to $\epsilon_0 \ln \frac{L}{r_0}$. This logarithmic divergence makes bare perturbation theory suspect, since a notionally small $\mathcal{O}(\epsilon_0)$ correction turns out to have a logarithmically diverging coefficient.

To extract useful information from the bare perturbation theory, it is therefore necessary to appeal to the Callan-Symanzik equation for the one-point function S, and use the fact that S is expected to have the general form noted earlier in Eq. (12). In order to make contact with our bare perturbation theory result, we expand this renormalization group prediction to first order in the bare coupling constant:

$$\begin{aligned} S &= \frac{F_0\left(\frac{r}{L}\right)}{\sqrt{L}}\left(1 - \frac{\pi}{2}\epsilon_0 \ln\frac{L}{r_0} + \ldots\right)\left[1 + \epsilon_0 R\left(\frac{r}{L}\right) + \ldots\right] \\ &\cong \frac{F_0\left(\frac{r}{L}\right)}{\sqrt{L}}\left[1 - \frac{\pi}{2}\epsilon_0 \ln\frac{L}{r_0} + \epsilon_0 R\left(\frac{r}{L}\right) + \ldots\right]. \end{aligned} \quad (13)$$

By comparing with the result of our first-order perturbation theory in ϵ_0, it becomes possible to fix the functions F_0 and R. This strategy gives us the one-loop RG improved result for the alternating part of $\langle S^z(r)\rangle_\uparrow$:

$$N_z(r) = c\sqrt{a}\frac{F_0}{\sqrt{L}}\left[\frac{\epsilon_0}{\epsilon(L)}\right]^{\frac{1}{4}}[1 + \epsilon(L)R], \quad (14)$$

with

$$F_0\left(\frac{r}{L}\right) = -\sqrt{\frac{\pi \sin\theta_r}{2}}, \quad (15)$$

and

$$R\left(\frac{r}{L}\right) = \frac{\pi}{2}\ln\frac{2\pi}{\sin\theta_r} + 2\left(\int_0^{\theta_r} + \int_0^{\pi-\theta_r}\right)\phi\cot\phi d\phi, \quad (16)$$

with $\theta_r \equiv \frac{\pi r}{L}$.

In order to cast this expression into an explicitly useful form for comparison with numerical results on a chain of N sites with lattice spacing a, we rewrite the prefactor as

$$\left[\frac{\epsilon_0}{\epsilon(L)}\right]^{\frac{1}{4}} \approx \left(1 + 2\pi|\epsilon_0|\left\{\ln\left(\frac{L}{r_0}\right) + \frac{1}{2}\ln\left[\ln\left(\frac{L}{r_0}\right)\right]\right\}\right)^{1/4}, \quad (17)$$

express $\epsilon(L)$ as

$$\epsilon(L) = -\frac{|\epsilon_0|}{1 + 2\pi|\epsilon_0|\left\{\ln\left(\frac{L}{r_0}\right) + \frac{1}{2}\ln\left[\ln\left(\frac{L}{r_0}\right)\right]\right\}}, \quad (18)$$

choose the short-distance cutoff as $r_0 = a$, and set the length L to $L = (N+1)a$ (see Sec. II C below). Equations (14)–(16) with these inputs constitutes a theoretical prediction with two free parameters (the overall amplitude c and the bare coupling ϵ_0 at the lattice scale), and we find below that this provides an extremely good two-parameter fit of our numerical data in the power-law ordered antiferromagnetic phase of the one-dimensional JQ_3 model. In addition, the spin texture at $q = q_c$, the critical end-point of this power-law ordered Néel phase, fits extremely well to the scaling function F_0, to which the more general prediction reduces when $\epsilon_0 = 0$.

What do these results tell us about the possible origins of such multiplicative logarithmic corrections to spin textures at other critical points, such as the deconfined quantum critical points alluded to in the introduction? To explore this, let us first consider the same calculation of the alternating part of the spin texture, but at some other critical point with an *irrelevant* coupling g with small scaling dimension α. In other words, we assume that $\beta(g) = -\alpha g + \ldots$ with α small and positive, and $\gamma(g) = \delta_0 + \delta_1 g + \ldots$. In this case, the Callan-Symanzik equation would predict that N_z satisfy the scaling law

$$N_z(\vec{r}) = \exp\left[-\int_{g_0}^{g(L)}\frac{\gamma(g)}{\beta(g)}dg\right]F_n\left[\frac{\vec{r}}{L}, g(L)\right] \quad (19)$$

for some function F_n (that needs a more detailed analysis to determine). Using the postulated form of the β and γ functions, one can therefore conclude

$$N_z(\vec{r}) = \frac{\mathcal{C}}{L^{\delta_0}}F_n\left(\frac{\vec{r}}{L}, g_0/L^\alpha\right). \quad (20)$$

Thus, if the critical point in question has no marginal operators, the alternating part of the spin texture will quite generally obey scaling as long as the scaling function $F_n(x,y)$ is well defined and nonzero in the $y \to 0$ limit. Conversely, if the critical point in question has a marginal operator, scaling will always be violated by multiplicative logarithmic factors even if the scaling function $F_n(x,y)$ is well defined and non zero in the $y \to 0$ limit. Indeed, in this marginal case, the only way of *evading* a multiplicative logarithmic correction would be to "arrange" for the $y \to 0$ limit of the

scaling function $F_n(x,y)$ to have exactly the "right" kind of singularity needed to cancel the effects of the multiplicative logarithmic correction coming from the exponential prefactor. One may therefore conclude that unless the scaling function has a particularly "fine-tuned" form, scaling predictions for N_z will be generically violated by multiplicative logarithmic corrections in the presence of a marginal operator. Conversely, irrelevant operators can lead to violations of scaling only if the scaling function is not well defined as this operator renormalizes to zero.

This should be contrasted with the *uniform* part $\langle L_z(\vec{r})\rangle$ of the spin texture at such a quantum critical point. Since the uniform part is the expectation value of a conserved charge [assuming SU(2) invariance of the underlying microscopic Hamiltonian], $\gamma(g)$ cannot acquire any corrections: $\gamma(g)=\delta_0$, a constant independent of g. With this change, it is clear that the prefactor in Eq. (19) always reduces to $L^{-\delta_0}$ independent of the form of $\beta(g)$, which encodes whether g is irrelevant or marginally irrelevant. In this case, there are no multiplicative logarithmic violations of scaling in the marginal case as long as long as the scaling function $F_u(x,y)$ for the uniform part is nonzero and well defined in the $y\to 0$ limit.

However, it is interesting to note that the marginality of g can have important consequences even in this case. For instance, in the one-dimensional example considered here, an elementary exercise shows that $F_u(r/L, y=0)$ is a constant independent of r/L. If one analyzes the texture in Fourier space, this implies that the scaling part of the uniform component vanishes at all nonzero wave vectors $q\neq 0$. As a result, the measured values at any nonzero wave vector near $q=0$ will not obey the q space version of the naive scaling ansatz, and their behavior will be dominated by the first term in the expansion of $F_u[r/L,\epsilon(L)]$ in powers of the renormalized coupling $\epsilon(L)$ that is going to zero logarithmically slowly as L is increased.

C. Details

When a missing-spin defect is introduced into a periodic spin chain of $N+1$ sites, it converts the system into a spin chain of N spins obeying open boundary conditions. These open boundary conditions can be modeled by referring back to the original periodic system and requiring that the spin density is constrained to go to zero at the missing site. As is well known,[24,25] this boundary condition can be incorporated by expanding the bosonic field ϕ in terms of bosonic normal modes as follows:

$$\phi(r) = \pi R + \frac{q_0}{L}r + \sum_{n=1}^{\infty}\frac{\sin\left(\frac{n\pi r}{L}\right)(a_n+a_n^\dagger)}{\sqrt{\pi n}},$$
$$\widetilde{\phi}(r) = \widetilde{\phi}_0 + i\sum_{n=1}^{\infty}\frac{\cos\left(\frac{n\pi r}{L}\right)(a_n-a_n^\dagger)}{\sqrt{\pi n}}. \tag{21}$$

Here, the nonzero bosonic commutation relations are $[\widetilde{\phi}(0),q_0]=i$,$[a_m,a_n^\dagger]=\delta_{mn}$, H_0 can be written [apart from an (infinite) constant $\frac{u}{2}\sum_{n=1}^{\infty}\frac{n\pi}{L}$] in the canonical form

$$H_0 = \frac{u}{2}\frac{q_0^2}{L} + \sum_{n=1}^{\infty}\left(\frac{un\pi}{L}\right)a_n^\dagger a_n. \tag{22}$$

Thus the ground state $|G_0\rangle$ of the unperturbed Hamiltonian is the vacuum for all the a_n and an eigenstate of the zero mode q_0. Indeed, $q_0|G_0\rangle=\pi R|G_0\rangle$ for the $S_{\rm tot}=1/2$, $S^z_{\rm tot}=1/2$ ground state that we wish to model (more generally $|G_0\rangle$ is an eigenstate of q_0 with eigenvalue $2\pi RS^z_{\rm tot}$).

Now, the ground state corrected to first order in ϵ_0 can be written formally as

$$|G\rangle \cong |G_0\rangle - \sum_{k\neq G_0}\left(\frac{\langle k|H_1|G_0\rangle}{E^0_k - E^0_{G_0}}\right)|k\rangle. \tag{23}$$

Here, $k\equiv\{N_n\}$ with $n=1,2\ldots,\infty$ and N_n being the number of bosons in mode n. For an arbitrary excited state, we have the unperturbed energy

$$E^0(\{N_n\}) = \frac{u}{2}\frac{q_0^2}{L} + \sum_n \omega_n N_n \tag{24}$$

with $\omega_n = un\pi/L$, which gives us the following expression for the energy denominators:

$$E^0(\{N_n\}) - E^0_g = \sum_n \omega_n N_n. \tag{25}$$

As a result, our formal expression for the ground state corrected to first order in ϵ_0 now reads

$$|G\rangle = |\{N_n=0\}\rangle + \frac{u\epsilon_0}{r_0^2} \times \sum_{\{N_n\}\neq\{0\}}\left(\frac{\langle\{N_n\}|\int_0^L\cos(\frac{2\phi(x)}{R})|\{0\}\rangle}{u\sum_n\frac{n\pi}{L}N_n}\right)|\{N_n\}\rangle. \tag{26}$$

This gives the following formal expression for the one point function:

$$S \cong \langle\{0\}|\frac{1}{\sqrt{r_0}}\sin\left[\frac{\phi(r)}{R}\right]|\{0\}\rangle + \frac{\epsilon_0}{r_0^2}\sum_{\{N_n\}\neq\{0\}}\frac{\langle\{0\}|\frac{1}{\sqrt{r_0}}\sin\left[\frac{\phi(r)}{R}\right]|\{N_n\}\rangle\langle\{N_n\}|\int_0^L dx\cos\left[\frac{2\phi(x)}{R}\right]|\{0\}\rangle}{\sum_n\frac{n\pi}{L}N_n}$$
$$+\frac{\epsilon_0}{r_0^2}\sum_{\{N_n\}\neq\{0\}}\frac{\langle\{N_n\}|\frac{1}{\sqrt{r_0}}\sin\left[\frac{\phi(r)}{R}\right]|\{0\}\rangle\langle\{0\}|\int_0^L dx\cos\left[\frac{2\phi(x)}{R}\right]|\{N_n\}\rangle}{\sum_n\frac{n\pi}{L}N_n}, \tag{27}$$

where we can set $R=1/\sqrt{2\pi}$ in the contributions that arise from the $\mathcal{O}(\epsilon_0)$ corrections to $|G_0\rangle$, as long as we are careful to use the full expression $R=(2\pi-2\pi^2\epsilon_0)^{-1/2}\approx(1+\pi\epsilon_0/2)/\sqrt{2\pi}$ when evaluating the first "unperturbed"

term in order to obtain the latter correct to $\mathcal{O}(\epsilon_0)$. To evaluate the matrix elements and expectation values, it is useful to write the state $|\{N_n\}\rangle$ in "coordinate" representation as

$$\langle\{y_n\}|\{N_n\}\rangle = \prod_{n=1}^{\infty}\left[\frac{1}{\pi^{\frac{1}{4}}2^{\frac{N_n}{2}}}\frac{1}{\sqrt{N_n!}}e^{-\frac{y_n^2}{2}}H_{N_n}(y_n)\right], \quad (28)$$

where the coordinates $y_n = \frac{a_n+a_n^\dagger}{\sqrt{2}}$ are conjugate to "momenta" $\pi_n = \frac{a_n-a_n^\dagger}{i\sqrt{2}}$ and $H_m(x)$ is the mth Hermite polynomial of x. The expectation values in our formal perturbative expression above can now be evaluated in closed form using this coordinate representation to obtain the following compact integral representation of S:

$$\begin{aligned} S\left(L,\frac{r}{L},\epsilon_0\right) &= -\sqrt{\frac{\pi\sin\theta_r}{2L}}\left(1-\frac{\pi\epsilon_0}{2}\ln\frac{\pi r_0}{2L\sin\theta_r}\right) \\ &-\epsilon_0\sqrt{\frac{\pi\sin\theta_r}{2L}}\frac{1}{4\sin\theta_r}\times\left\{\int_0^\infty\int_0^\pi dsd\phi\frac{\sin(\theta_r-2\phi)}{\sin^2\phi}\left[\frac{\cos(\theta_r-\phi)-\cos(\theta_r+\phi)}{\cosh s-\cos(\theta_r-\phi)}\right]\right\} \\ &-\epsilon_0\sqrt{\frac{\pi\sin\theta_r}{2L}}\frac{1}{4\sin\theta_r}\times\left\{\int_0^\infty\int_0^\pi dsd\phi\frac{\sin(\theta_r+2\phi)}{\sin^2\phi}\int_0^\infty ds\left[\frac{\cos(\theta_r+\phi)-\cos(\theta_r-\phi)}{\cosh s-\cos(\theta_r+\phi)}\right]\right\}. \end{aligned} \quad (29)$$

Here, $\theta_r \equiv \pi r/L$, and we have regulated mode sums $\sum_{m=1}^{\infty} g_m$ over the harmonic oscillator modes by replacing them with $\sum_{m=1}^{\infty} g_m \exp(-\pi m r_0/L)$ whenever necessary. It is now possible to do the s integrals in closed form to obtain the following integral representation for S:

$$\begin{aligned} S\left(L,\frac{r}{L},\epsilon_0\right) &= -\sqrt{\frac{\pi\sin\theta_r}{2L}}\left(1-\frac{\pi\epsilon_0}{2}\ln\frac{\pi r_0}{2L\sin\theta_r}\right)+\frac{\epsilon_0}{2}\left(\frac{\pi}{2L}\right)^{\frac{1}{2}}\int_0^{\pi-\theta_r}d\phi\frac{2\sin\phi\sin\theta_r}{\sqrt{\sin\theta_r}\sin^2\phi}\sin(2\phi+\theta_r)\frac{\pi-(\phi+\theta_r)}{\sin(\pi-(\phi+\theta_r))} \\ &+\frac{\epsilon_0}{2}\left(\frac{\pi}{2L}\right)^{\frac{1}{2}}\left\{\int_{\pi-\theta_r}^{\pi}d\phi\frac{2\sin\phi\sin\theta_r}{\sqrt{\sin\theta_r}\sin^2\phi}\sin(2\phi+\theta_r)\frac{(\phi+\theta_r)-\pi}{\sin[(\phi+\theta_r)-\pi]}\right. \\ &\left.+\int_0^{\theta_r}d\phi\frac{2\sin\phi\sin\theta_r}{\sqrt{\sin\theta_r}\sin^2\phi}\sin(2\phi-\theta_r)\frac{(\phi-\theta_r)+\pi}{\sin[(\phi-\theta_r)+\pi]}\right\} \\ &+\frac{\epsilon_0}{2}\left(\frac{\pi}{2L}\right)^{\frac{1}{2}}\int_{\theta_r}^{\pi}d\phi\frac{2\sin\phi\sin\theta_r}{\sqrt{\sin\theta_r}\sin^2\phi}\sin(2\phi-\theta_r)\frac{\pi-(\phi-\theta_r)}{\sin[\pi-(\phi-\theta_r)]}. \end{aligned} \quad (30)$$

This integral representation is again regulated with the short distance cut-off r_0 by requiring that the ϕ integrals are to be done by excluding the region $[\theta_r-\pi r_0/L,\theta_r+\pi r_0/L]$ from the integration range. Somewhat remarkably, it is possible to obtain explicit expressions for all integrals sensitive to this ultraviolet cutoff, and thereby reduce this integral representation to the following compact and simple form:

$$\begin{aligned} S\left(L,\frac{r}{L},\epsilon_0\right) &= -\sqrt{\frac{\pi\sin\theta_r}{2L}}\left[1-\frac{\pi\epsilon_0}{2}\ln\frac{L}{r_0}+\frac{\pi\epsilon_0}{2}\ln\frac{2\pi}{\sin\theta_r}\right. \\ &\left.+2\epsilon_0\left(\int_0^{\theta_r}+\int_0^{\pi-\theta_r}\right)\phi\cot\phi d\phi\right]. \end{aligned} \quad (31)$$

Comparing with the general expectation from our RG analysis [Eq. (13)], we therefore obtain

$$F_0\left(\frac{r}{L}\right) = -\sqrt{\frac{\pi\sin\theta_r}{2}}. \quad (32)$$

and

$$R\left(\frac{r}{L}\right) = \frac{\pi}{2}\ln\frac{2\pi}{\sin\theta_r}+2\left(\int_0^{\theta_r}+\int_0^{\pi-\theta_r}\right)\phi\cot\phi d\phi, \quad (33)$$

as already advertised in Sec. II B.

III. NUMERICAL COMPUTATIONS

Our numerical work on chains with an odd number of sites relies crucially on the spin-half sector generalization[22] of the valence-bond projector QMC algorithm.[21] In our approach, the $S_{\rm tot} = 1/2$ sector of the Hilbert space of an odd number of $S = 1/2$ moments, to which the ground state belongs, is spanned by a bipartite valence-bond cover that leaves one spin "free." Roughly speaking, the ground-state spin texture $\Phi(r) = \langle S^z(r)\rangle_\uparrow$ is then obtained directly in our method by keeping track of the probability for the free spin to be at various sites r (see Ref. 22 for details).

This method provides an extremely efficient means of accessing ground-state properties at large sizes as long as the Hamiltonian is *unfrustrated*. It has been used in computations of ground-state spin textures at deconfined critical points in two-dimensional SU(2) and SU(3) antiferromagnets[14,19] as well as in very recent parallel work on developing a diagnostic for the presence of sharply defined spinon excitations[26] in antiferromagnets.

We consider pure systems with periodic boundary conditions and total number of sites ranging from $N = 60$ to 960 as well as the corresponding open spin chains obtained by removing one site from the pure system. Our projection power

is chosen to scale as $4N^3$ to ensure convergence to the ground state. We perform $\gtrsim 10^5$ equilibration steps followed by $\gtrsim 10^6$ Monte Carlo measurements to ensure that statistical errors are under control. In systems with a vacancy, we measure $\Phi(r)$ in the manner outlined above, and coarse-grain over pairs of successive sites to obtain our numerical results for the alternating part $N_z(r)$, which is to be thought of as living on bond-centers in this coarse-graining procedure. We have checked that our conclusions are not sensitive to the precise coarse-graining procedure used, although nonuniversal details, such as the overall amplitude of $N_z(r)$, do change.

For the corresponding pure systems, we employ the singlet sector valence bond projection QMC technique,[21] and calculate the ground-state spin-spin correlation function $C(j) = \langle \vec{S}(0) \cdot \vec{S}(j) \rangle$ for two sites separated by $j-1$ intervening sites ($j \leqslant N/2$, where N is the total number of spins). To begin with, we scan the six-spin coupling $q = Q/4J$ and study the q and N dependence of $NC(N/2)$ as a convenient diagnostic that distinguishes the power-law Néel ordered phase at small q from the spontaneously dimerized VBS ordered phase that is stabilized for large q. In the power-law Néel phase, $NC(N/2)$ grows (logarithmically) slowly with N, while in the VBS phase, it falls off rapidly with increasing N. Precisely at the critical point separating these two phases, we thus expect a crossing point for $NC(N/2)$ plotted against q for various values of N. This is precisely what is seen in our data shown in Fig 1. From our data, we estimate that the critical point separating these two phases is located at $q_c \approx 0.04$ with an error of approximately 0.005 estimated by extrapolating for the position of the crossing point (this estimate is consistent with the critical point found in Ref. 26).

With this in hand, we compute the ground state spin texture in the corresponding chains with one site removed for several $q \leqslant q_c$ for a range of system sizes. The alternating part of the computed spin texture is then compared with the scaling predictions obtained by setting $\epsilon_0 = 0$ as well as with our RG improved perturbation theory predictions. The former

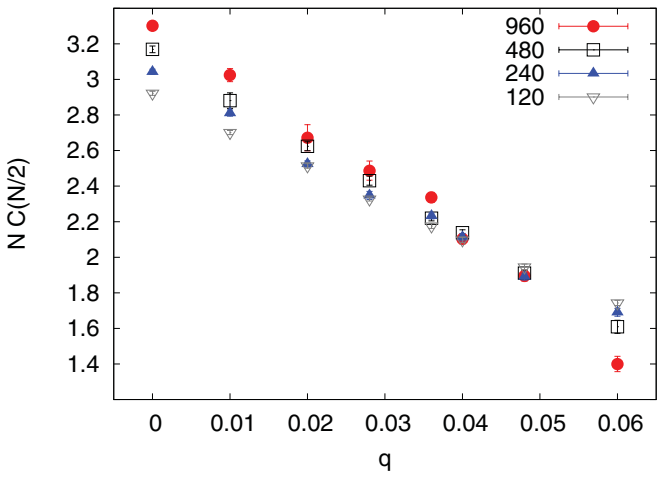

FIG. 1. (Color online) Spin-spin correlation function at distance $N/2$ $C(N/2) = \langle \vec{S}_i \cdot \vec{S}_{i+N} \rangle$ in the ground state of a periodic chain with N spins, multiplied by N and plotted against q to serve as diagnostic of the quantum phase transition from power-law Néel order to valence-bond solid order, as discussed in the text.

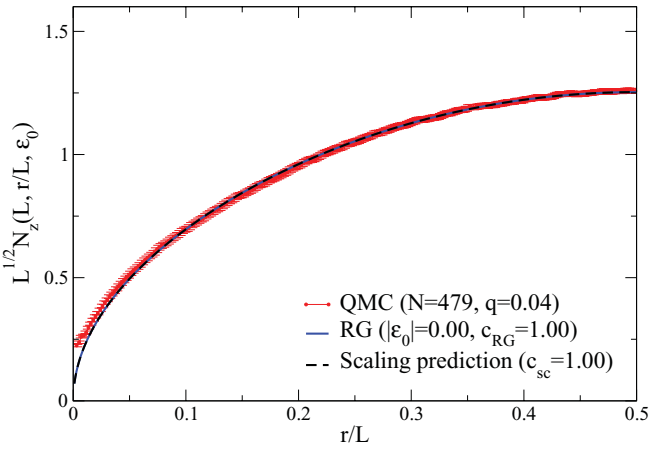

FIG. 2. (Color online) $L^{1/2}N_z(r)$ plotted vs r/L (where $L = N+1$ for chains with $N = 479$ spins and open boundary conditions) and compared with the scaling prediction F_0 for $q = 0.04$, the approximate location of the quantum critical point separating the power-law Néel phase from the VBS ordered phase in the one-dimensional JQ_3 model. Note the data fit essentially perfectly to the scaling prediction with the same prefactor c_{sc} as in the next figure that displays analogous data for $N = 959$. Also note that the best two-parameter fit corresponding to our RG improved perturbation theory result also gives $|\epsilon_0| = 0$, and thus coincides with the scaling answer.

represents a one-parameter fit of the data, with the overall amplitude c being the only free parameter, while the latter should be thought of as a two parameter fit, with the bare value ϵ_0 of the sine-Gordon coupling being the second fitting parameter.

In Figs. 2 and 3, we first display our data for the alternating part of the spin texture and compare it with the scaling prediction at the putative critical point $q = q_c$ for two of our largest system sizes. As is clear from these two figures, the scaling prediction fits extremely well to all the data at both sizes. Furthermore, a two-parameter fit using the RG-improved perturbation theory result yields a best-fit value of ϵ_0 indistinguishable from $\epsilon_0 = 0$. This confirms our identification of the critical point, since we expect that the bare coefficient of the marginally irrelevant cosine interaction is zero at this quantum phase transition.

This excellent fit to the scaling prediction should be contrasted with the results shown in Figs. 4–7, which show numerical results at two representative points in the power-law Néel phase compared with the one-parameter fit obtained from the scaling prediction. As is clear from these figures, the scaling prediction simply cannot provide a satisfactory account of the data for $q < q_c$, with the discrepancy being more pronounced for smaller q, that is, *further away* from the critical point. Furthermore, the observed deviations from scaling cannot be simply ascribed to an overall N-dependent prefactor that grows with system size, since the *shapes* of the curves are themselves slightly different from the scaling prediction.

In the same figures, we also show the best two-parameter fit obtained by using our RG improved perturbation theory result. Two points are worth noting regarding these two parameter fits: firstly, the best-fit values of $|\epsilon_0|$ increase as one goes further

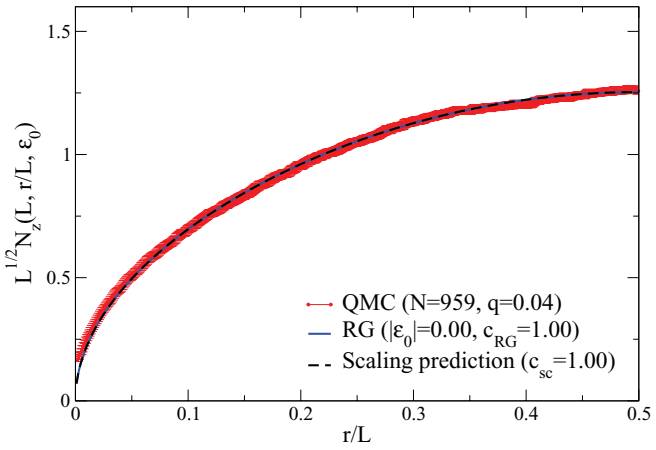

FIG. 3. (Color online) $L^{1/2}N_z(r)$ plotted vs r/L (where $L = N + 1$ for chains with $N = 959$ spins and open boundary conditions) and compared with the scaling prediction F_0 for $q = 0.04$, the approximate location of the quantum critical point separating the power-law Néel phase from the VBS ordered phase in the one-dimensional JQ_3 model. Note the data fit essentially perfectly to the scaling prediction with the same prefactor c_{sc} that was used in the earlier figure for $N = 479$. Also note that the best two-parameter fit corresponding to our RG improved perturbation theory result also gives $|\epsilon_0| = 0$, and thus coincides with the scaling answer.

away from $q = q_c$, consistent with the expectation that the bare coefficient of the cosine interaction vanishes as q approaches q_c. Second, the RG improved perturbation theory provides a much better fit at $q = 0.02$ than at the Heisenberg point $q = 0$—again, this is consistent with our expectations, since our calculation is perturbative in the renormalized coupling $\epsilon(L)$, and is therefore expected to provide a better approximation when the bare value of $|\epsilon_0|$ is smaller to begin with.

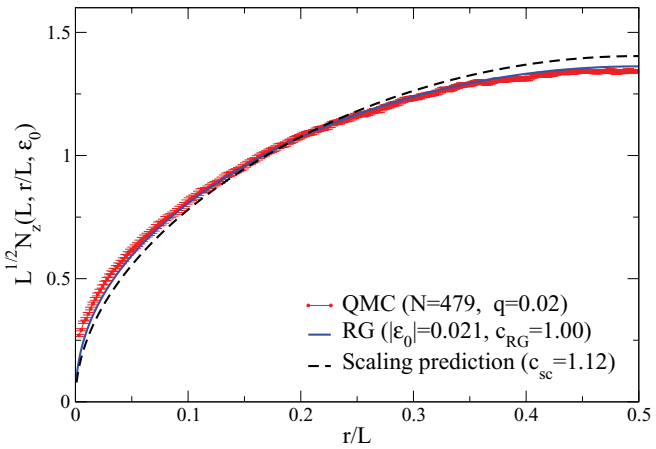

FIG. 4. (Color online) $L^{1/2}N_z(r)$ plotted vs r/L in the power-law ordered Néel phase at $q = 0.02$ (where $L = N + 1$ for chains with $N = 479$ spins and open boundary conditions) and compared with the scaling prediction with a common best fit prefactor c_{sc} (which is also used in the next figure for $N = 959$ data). Note that the deviation of the data from the scaling prediction cannot be simply ascribed to an overall multiplicative factor that grows with N, since the *shape* of the curves is slightly different. The data are also fit to the best two-parameter fit corresponding to our RG improved perturbation theory result, and the agreement is seen to be excellent for the best common fit values (also used in the next figure for $N = 959$ data) of c_{RG} and $|\epsilon_0|$ listed in the legend.

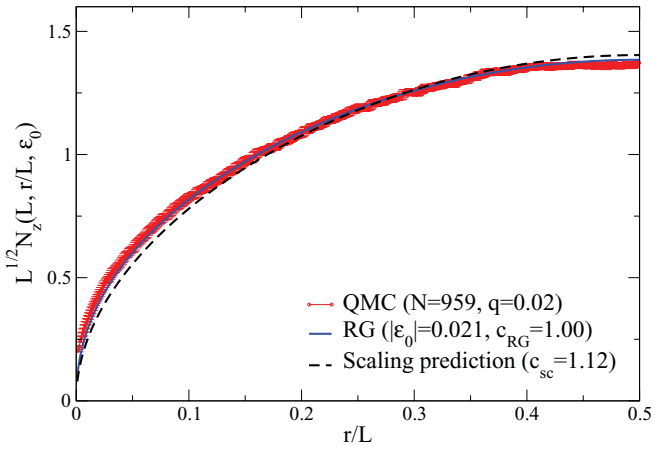

FIG. 5. (Color online) $L^{1/2}N_z(r)$ plotted vs r/L in the power-law ordered Néel phase at $q = 0.02$ (where $L = N + 1$ for chains with $N = 959$ spins and open boundary conditions) and compared with the scaling prediction with a common best fit prefactor c_{sc} (which was also used in the previous figure for $N = 479$ data). Note that the deviation of the data from the scaling prediction cannot be simply ascribed to an overall multiplicative factor that grows with N, since the *shape* of the curves is slightly different. Data at both sizes are also fit to the best two-parameter fit corresponding to our RG improved perturbation theory result, and the agreement is seen to be excellent for the best choice of N independent values for c_{RG} and $|\epsilon_0|$ listed in the legend.

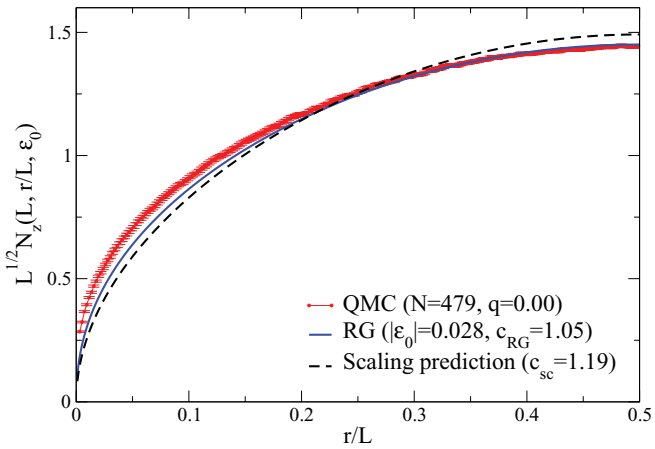

FIG. 6. (Color online) $L^{1/2}N_z(r)$ plotted vs r/L in the power-law ordered Néel phase at $q = 0$ (where $L = N + 1$ for chains with $N = 479$ spins and open boundary conditions) and compared with the scaling prediction with a common best fit prefactor c_{sc} (which is also used in the next figure for $N = 959$ data). Note that the deviation of the data from the scaling prediction cannot be simply ascribed to an overall multiplicative factor that grows with N, since the *shape* of the curves is slightly different. The data are also fit to the best two-parameter fit corresponding to our RG improved perturbation theory result, and the agreement is seen to be excellent for the best common fit values (also used in the next figure for $N = 959$ data) of c_{RG} and $|\epsilon_0|$ listed in the legend.

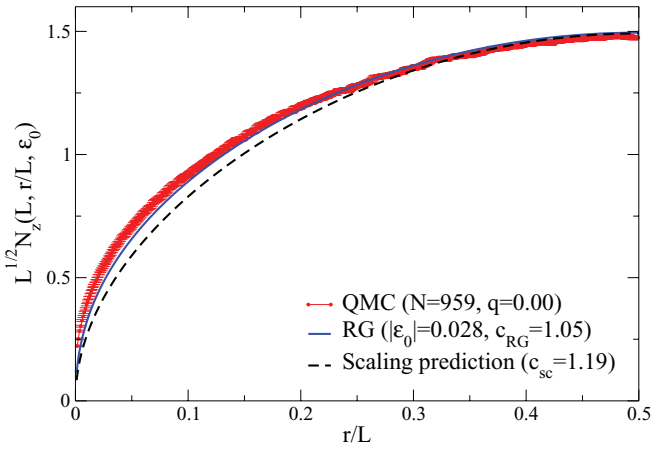

FIG. 7. (Color online) $L^{1/2}N_z(r)$ plotted vs r/L in the power-law ordered Néel phase at $q = 0.0$ (where $L = N + 1$ for chains with $N = 959$ spins and open boundary conditions) and compared with the scaling prediction with a common (N independent) best-fit prefactor c_{sc}. Note that the deviation of the data from the scaling prediction cannot be simply ascribed to an overall multiplicative factor that grows with N, since the *shape* of the curves is slightly different. Data at both sizes is also fit to the best two-parameter fit corresponding to our RG improved perturbation theory result, and the agreement is seen to be quite reasonable, but not perfect, for the best common (N independent) fit values of c_{RG} and $|\epsilon_0|$ listed in the legend.

IV. DISCUSSION

We first discuss the relationship of our calculations with earlier calculations of the effect of vacancies on[27–30] spin chains. These have typically focused on inpurity effects in the low-field NMR Knight shift and relaxation rate $1/T_1$, or on the impurity contribution to the linear spin susceptibility and zero-field spin structure factor of such chains. All these experimental observables probe the spin correlations of the system in the absence of an external magnetic field. In contrast, our results focus on local spin texture induced by the presence of vacancies *at* $T = 0$, which is a different quantity. This difference is clear when one considers the dependence of the NMR Knight-shift K on $g\mu_B B/k_B T$, the ratio of the Zeeman energy to $k_B T$: for $g\mu_B B/k_B T \ll 1$, $K \propto \chi_{\rm loc}(T)B$, where $\chi_{\rm loc}(T)$ is the local susceptibility of the spin system at temperature T. This is, for instance, the quantity focused on in Ref 27. On the other hand, in the opposite low-temperature limit $g\mu_B B/k_B T \gg 1$, a better approximation to K is obtained by computing $\langle S^z(\vec{r})\rangle_{T=0}$, the local spin polarization induced by an external magnetic field B at $T = 0$. This is the impurity spin texture we have focused on in this paper—in our case, the ground state of the system with an impurity is a doublet, and introducing a nonzero field B at $T = 0$ is equivalent to performing all computations in the the $S^z_{\rm tot} = +1/2$ ground state, as we have done. This distinction between the high-field (low-temperature) and low-field (high-temperature) regimes is of course well known, and has been emphasized earlier in the context of $1/T_1$ measurements in Haldane-gapped spin chains, where the corresponding distinction between the high field (low temperature) and low field (high temperature) behavior of $1/T_1$ is related respectively to the high-frequency collisionless and low-frequency diffusive regimes of the spin-spin autocorrelation function.[31,32]

Second, we note that although we have focused on a specific model with six-spin interactions that destabilize the power-law ordered Néel phase of the spin-1/2 Heisenberg model, our analytical results on the logarithmic corrections to the impurity spin texture are more general. Indeed, our six-spin interactions were chosen to ensure that the low-energy, long-distance physics of our system is the same as that of a much more physical system, namely the Heisenberg spin chain with nearest-neighbor exchange J_1 and next-nearest-neighbor exchange J_2. Therefore our analytical results can equally well be viewed as statements about impurity spin textures in this J_1-J_2 chain. Finally, we note that a Jordan-Wigner transformation connects our spin textures to Friedel oscillations in a Luttinger liquid,[33,34] and some of our results on logarithmic corrections may be carried over.[35]

ACKNOWLEDGMENTS

We acknowledge useful discussions with Ribhu Kaul, Nicolas Laflorencie, Gautam Mandal, Anders Sandvik, and Diptiman Sen, computational resources of the TIFR, and support from DST (India) grant DST-SR/S2/RJN-25/2006 and Indo-French Centre for the Promotion of Advanced Research (IFCPAR/CEFIPRA) Grant No. 4504-1.

[1] M. Takigawa, N. Motoyama, H. Eisaki, and S. Uchida, Phys. Rev. B **55**, 14129 (1997).
[2] B. Lake, D. A. Tennant, C. D. Frost, and S. E. Nagler, Nat. Mater. **4**, 329 (2005).
[3] B. Lake, D. A. Tennant, and S. E. Nagler, Phys. Rev. B **71**, 134412 (2005).
[4] I. Affleck, *Fields, Strings, and Critical Phenomena*, edited by E. Brezin and J. Zinn-Justin (North-Holland, Amsterdam, 1990).
[5] R. R. P. Singh, M. E. Fisher, and R. Shankar, Phys. Rev. B **39**, 2562 (1989).
[6] I. Affleck, D. Gepner, H. Shultz, and T. Ziman, J Phys. A: Math. Gen. **22**, 511 (1989).
[7] V. Barzykin and I. Affleck, J Phys. A: Math. Gen. **32**, 867 (1999).
[8] E. Orignac, Eur. Phys. J. B **39**, 335 (2004).
[9] R. Chitra, S. Pati, H. R. Krishnamurthy, D. Sen, and S. Ramasesha, Phys. Rev. B **52**, 6581 (1995).
[10] S. Eggert, Phys. Rev. B **54**, R9612 (1996).
[11] R. Kenna, Nucl. Phys. B **691 [FS]**, 292 (2004).
[12] S. Sachdev, Phys. Rev. B **50**, 13006 (1994).
[13] A. W. Sandvik, Phys. Rev. Lett. **104**, 177201 (2010).
[14] A. Banerjee, K. Damle, and F. Alet, Phys. Rev. B **82**, 155139 (2010).
[15] T. Senthil, L. Balents, S. Sachdev, A. Vishwanath, and M. P. A. Fisher, Phys. Rev. B **70**, 144407 (2004).
[16] A. W. Sandvik, Phys. Rev. Lett. **98**, 227202 (2007).
[17] R. K. Kaul, Phys. Rev. B **84**, 054407 (2011).

[18] A. W. Sandvik, V. N. Kotov, and O. P. Sushkov, Phys. Rev. Lett. **106**, 207203 (2011).
[19] A. Banerjee, K. Damle, and F. Alet, Phys. Rev. B **83**, 235111 (2011).
[20] J. Lou, A. W. Sandvik, and N. Kawashima, Phys. Rev. B **80**, 180414(R) (2009).
[21] A. W. Sandvik and H. G. Evertz, Phys. Rev. B **82**, 024407 (2010).
[22] A. Banerjee and K. Damle, J. Stat. Mech. (2010) P08017.
[23] J. V. José, L. P. Kadanoff, S. Kirkpatrick, and D. R. Nelson, Phys. Rev. B **16**, 1217 (1977).
[24] T. Hikihara and A. Furusaki, Phys. Rev. B **63**, 134438 (2001).
[25] S. Eggert and I. Affleck, Phys. Rev. B **46**, 10866 (1992).
[26] Y. Tang and A. W. Sandvik (unpublished).
[27] J. Sirker and N. Laflorencie, Europhys. Lett. **86**, 57004 (2009).
[28] S. Eggert and I. Affleck, Phys. Rev. Lett. **75**, 934 (1995).
[29] V. Brunel, M. Bocquet, and Th. Jolicoeur, Phys. Rev. Lett. **83**, 2821 (1999).
[30] S. Fujimoto and S. Eggert, Phys. Rev. Lett. **92**, 037206 (2004).
[31] S. Sachdev and K. Damle, Phys. Rev. Lett. **78**, 943 (1997).
[32] K. Damle and S. Sachdev, Phys. Rev. B **57**, 8307 (1998).
[33] R. Egger and H. Grabert, Phys. Rev. Lett. **75**, 3505 (1995).
[34] G. Bedürftig, B. Brendel, H. Frahm, and R. M. Noack, Phys. Rev. B **58**, 10225 (1998).
[35] We wish to thank one of the referees for pointing this out.